INFECTION AND IMMUNITY, June 2006, p. 3576–3586 Vol. 74, No. 6
0019-9567/06/$08.00+0 doi:10.1128/IAI.01262-05

Identification of *Burkholderia pseudomallei* Genes Required for the Intracellular Life Cycle and In Vivo Virulence

Sabine Pilatz,[1] Katrin Breitbach,[1,2] Nadine Hein,[1,2] Beate Fehlhaber,[1] Jessika Schulze,[1] Birgit Brenneke,[1] Leo Eberl,[3] and Ivo Steinmetz[1,2]*

Institute of Medical Microbiology, Hannover Medical School, Carl-Neuberg-Str. 1, 30625 Hannover, Germany[1]; Friedrich Loeffler Institute for Medical Microbiology, Ernst Moritz Arndt University Greifswald, Martin-Luther-Strasse 6, 17487 Greifswald, Germany[2]; and Department of Microbiology, Institute of Plant Biology, University of Zürich, Zollikerstrasse 107, 8008 Zürich, Switzerland[3]

Received 4 August 2005/Returned for modification 19 October 2005/Accepted 27 February 2006

The bacterial pathogen *Burkholderia pseudomallei* invades host cells, escapes from endocytic vesicles, multiplies intracellularly, and induces the formation of actin tails and membrane protrusions, leading to direct cell-to-cell spreading. This study was aimed at the identification of *B. pseudomallei* genes responsible for the different steps of this intracellular life cycle. *B. pseudomallei* transposon mutants were screened for a reduced ability to form plaques on PtK2 cell monolayers as a result of reduced intercellular spreading. Nine plaque assay mutants with insertions in different open reading frames were selected for further studies. One mutant defective in a hypothetical protein encoded within the Bsa type III secretion system gene cluster was found to be unable to escape from endocytic vesicles after invasion but still multiplied within the vacuoles. Another mutant with a defect in a putative exported protein reached the cytoplasm but exhibited impaired actin tail formation in addition to a severe intracellular growth defect. In four mutants, the transposon had inserted into genes involved in either purine, histidine, or *p*-aminobenzoate biosynthesis, suggesting that these pathways are essential for intracellular growth. Three mutants with reduced plaque formation were shown to have gene defects in a putative cytidyltransferase, a putative lipoate-protein ligase B, and a hypothetical protein. All nine mutants proved to be significantly attenuated in a murine model of infection, with some mutants being essentially avirulent. In conclusion, we have identified a number of novel major *B. pseudomallei* virulence genes which are essential for the intracellular life cycle of this pathogen.

The environmental saprophyte *Burkholderia pseudomallei* is the causative agent of melioidosis, an infectious disease of humans and animals which is known to be a major cause of morbidity and mortality in certain areas of the tropics (45). In endemic areas, the bacterium can be isolated from soil and surface waters (10, 20). In most cases, humans and animals are thought to acquire the infection by inoculation of environmental organisms into minor cuts or abrasions or by inhalation after contact with water or soil (9). The clinical manifestations are extremely variable, ranging from inapparent infections to localized subacute or chronic infections and fulminant septicemias with abscesses in multiple organs (24). Severe pneumonia and septicemia with high mortality are the most common clinical presentations of melioidosis in northeastern Thailand and northern Australia (5, 8). *B. pseudomallei* has an extremely broad host range. Besides humans, infections have been reported for many species, ranging from rodents to pigs, sheep, goats, horses, birds, and reptiles (6). Recently, *B. pseudomallei* has been included on a list of potential biothreat agents as a category B agent (33).

Studies of the molecular basis of *B. pseudomallei* virulence have identified the type II O-PS moiety of the lipopolysaccharide and a capsular polysaccharide as contributors to virulence in various animal models (12, 32). By using a *Caenorhabditis elegans* model, Gan et al. identified virulence genes which seem to be of relevance in mice also, although their role in pathogenesis still needs to be determined (13). Moreover, LuxI and LuxR homologs of the highly complex quorum-sensing circuitry operating in *B. pseudomallei* contribute to the virulence of the organism. However, the virulence factors regulated by quorum sensing are not yet identified (35, 43, 44).

B. pseudomallei is a facultatively intracellular organism which is able not only to invade phagocytic and nonphagocytic cells but also to grow intracellularly (22, 30). It was demonstrated that *B. pseudomallei* can induce actin rearrangement initiated at one pole of the bacterium, leading to actin tail formation and actin-associated peripheral membrane protrusions causing intercellular spreading (4, 23). We recently analyzed the contributions of cytoskeletal proteins to *B. pseudomallei*-induced actin tail assembly. Our results implicate that the Arp2/3 complex is incorporated into *B. pseudomallei* actin tails, but overexpression of an Arp2/3 binding fragment of the Scar1 protein, shown previously to block the actin-based motility of *Listeria*, had no effect on *B. pseudomallei* tail formation. This study also indicated that *B. pseudomallei* actin-based motility occurs independently of the N-WASP and Ena/Vasp proteins. It therefore seems likely that the intracellular actin-based motility of *B. pseudomallei* is based on a mechanism which differs from those previously described for the microbial pathogens *Listeria*, *Shigella*, and vaccinia virus (4). A recent study identified a proline-rich putative autosecreted *B. pseudomallei* protein (BimA) that is required for *B. pseudo-*

* Corresponding author. Mailing address: Friedrich Loeffler Institute for Medical Microbiology, Ernst Moritz Arndt University Greifswald, Martin-Luther-Strasse 6, 17489 Greifswald, Germany. Phone: 49 3834-865587. Fax: 49 3834-865561. E-mail: steinmetz.ivo@uni-greifswald.de.

mallei actin-based motility. Although, BimA weakly activates actin polymerization in vitro in an Arp2/3-independent manner (40), it cannot be excluded that BimA stimulates actin tail formation via Arp2/3 in vivo. The requirement for the Arp2/3 complex in the actin-based motility of *B. pseudomallei* requires further study (4, 40), and the role of BimA in *B. pseudomallei* virulence needs to be determined.

Recently, a *B. pseudomallei* type III protein secretion system that shows similarities to the *Salmonella enterica* Inv/Spa/Prg-like type III system was identified (3, 31). Mutations affecting components of this type III secretion and translocation apparatus, termed Bsa, impair intracellular survival and prevent the escape of *B. pseudomallei* from endocytic vacuoles (41). It has recently been reported that the Bsa-secreted guanine nucleotide exchange factor BopE, with homologies to the *Salmonella* SopE/SopE2 proteins, contributes to invasion of *B. pseudomallei* into HeLa cells (37). However, the effector proteins involved in events subsequent to invasion, namely, the escape from the vacuole, intracellular survival, and growth, are unknown (38). In this study, we present an experimental system which enabled us to identify several *B. pseudomallei* genes which are relevant at different stages of the *B. pseudomallei* intracellular life cycle and represent major virulence factors of this organism.

MATERIALS AND METHODS

Bacterial strains and media. The *B. pseudomallei* non-L-arabinose-assimilating strain E8 comprises a soil isolate from the surrounding area of Ubon Ratchatani, Northeast Thailand (46), and was obtained from N. J. White (Faculty of Tropical Medicine, Mahidol University, Bangkok, Thailand). Bacteria were grown on Columbia agar, Ashdown agar (1), or Luria-Bertani (LB) agar plates, with or without antibiotics, at 37°C for 24 h. LB broth or modified Vogel-Bonner broth (3.3 mM $MgSO_4$, 10 mM citric acid, 28 mM $NaNH_4HPO_4$, 37 mM K_2HPO_4, 214 mM D-gluconic acid, pH 7.4) was used as liquid medium. When appropriate, antibiotics were added at the following concentrations: 25 μg/ml chloramphenicol, 25 μg/ml kanamycin, and 12.5 μg/ml tetracycline for *Escherichia coli* SM10(pOT182) and 100 μg/ml streptomycin and 50 μg/ml tetracycline for *B. pseudomallei* Tn*5*(pOT182) mutants. The growth of mutants and the wild type (WT) was compared in either LB broth or modified Vogel-Bonner broth during late exponential phase by measuring the optical density at 650 nm (OD_{650}). Differences in ODs of >0.2 between the wild type and mutants were considered significant. Complemented mutants were selected on agar containing 50 μg/ml tetracycline and 100 μg/ml trimethoprim. For supplementation experiments with prototrophic and auxotrophic mutants, bacteria were inoculated in modified Vogel-Bonner medium at an OD_{650} of 0.01, together with the respective supplements, and incubated at 37°C. Purines, pyrimidines, amino acids, and *para*-aminobenzoic acid (PABA) were all purchased from Sigma.

Cell culture and media. The PtK2 epithelial and J774A.1 macrophage cell lines were cultivated in Dulbecco's modified Eagle's medium (Biochrom, Berlin, Germany) supplemented with 10% fetal calf serum at 37°C in an atmosphere with 5% CO_2. HeLa cells were cultivated in minimum essential medium-Earle's medium (Biochrom, Berlin, Germany) supplemented with 2 mM glutamine, 0.1 mM nonessential amino acids, 1 mM sodium pyruvate, and 10% fetal calf serum at 37°C in an atmosphere with 5% CO_2.

General DNA methods. Transformation of *E. coli* was performed essentially as described previously (33a). Plasmid DNA was isolated with a plasmid preparation kit, and genomic DNA from *B. pseudomallei* was prepared by using a DNeasy tissue kit (both purchased from QIAGEN). DNA fragments were purified using a DNA and Gel Band purification kit from Amersham Pharmacia. PCR was performed using *Pfu*-Turbo DNA polymerase (Stratagene). All enzymes for restriction digestion and ligation were purchased from New England Biolabs and were used according to the manufacturer's instructions.

***B. pseudomallei* Tn*5*-OT182 mutagenesis and plaque assay screening.** *B. pseudomallei* E8 was mutagenized with Tn*5*-OT182 as described previously (11), with minor modifications. The donor strain, *E. coli* SM10(pOT182), was grown at 37°C in antibiotic-containing LB broth overnight, and the recipient strain, *B. pseudomallei* E8, was grown at 42°C on Columbia agar overnight. Instead of using a membrane filter mating technique, suspensions of donor and recipient strains were directly mixed together and plated on Columbia agar plates (approximately 3×10^6 CFU of the recipient and 3×10^7 CFU of the donor per plate) for mating at 37°C overnight. The bacterial lawn of each plate was harvested using 0.9% NaCl, and aliquots were plated on antibiotic-containing plates for isolation of Tn*5* mutants.

For plaque assay screening, 2.5×10^5 PtK2 cells were seeded in 12-well dishes 20 h prior to infection and grown to confluence. Individual Tn*5* mutants were cultivated in 48-well plates containing 500 μl LB broth per well. One-hundred-microliter samples of 1:100 dilutions of the bacterial suspensions were transferred to the 12-well dishes with PtK2 monolayers and incubated for 1 to 2 h to allow bacterial entry. PtK2 cells were washed twice with 0.01 M sodium phosphate buffer made isotonic with saline at pH 7.4 (PBS), and an agarose overlay consisting of Dulbecco's modified Eagle's medium (without phenol red) with 0.5% agarose and 250 μg kanamycin per ml was added to each well. Mutants were observed for reduced or delayed plaque formation compared to the *B. pseudomallei* wild type at 24 h and 48 h postinfection.

Molecular analysis of Tn*5*-OT182 mutants. The DNAs flanking Tn*5*-OT182 integrations were identified by self-cloning as described previously (11), with minor modifications. Briefly, 5 μg of mutant chromosomal DNA was digested overnight with restriction enzymes. DNA fragments (0.5 to 1.0 μg) were ligated in 200 μl buffer. After purification, 2 to 5 μl of the resulting 50-μl mixture was transformed into *E. coli* DH5α. The plasmids of successfully transformed *E. coli* cells were prepared as described above. To initiate DNA sequencing reactions with plasmids obtained by EcoRI self-cloning, the oligonucleotide OT182-RT (5′-ACA TGG AAG TCA GAT CCT GG-3′) was used. DNA sequences were analyzed using the latest Internet annotation from the *B. pseudomallei* genome sequencing project performed at the Sanger Institute (http://www.sanger.ac.uk/Projects/B_pseudomallei/).

Complementation in *trans* of *B. pseudomallei* mutants 25:90, 54:55, 56:65, and 1:4. For mutant 25:90, the forward primer BF55 (5′-GCTCTAGACAGAT ACAGCAGGCGCTCTTCGAG-3′) and the reverse primer BF24 (5′-AGA AAGCTTCAGCCGCTACTGCTGCTGCTTTTG-3′) (XbaI and HindIII restriction sites are underlined) were used to amplify a 1,093-bp fragment from *B. pseudomallei* E8 genomic DNA containing the BPSL1528 coding region plus 337 bp upstream of the translational start and 6 bp downstream of the stop codon. Following digestion with XbaI and HindIII, this fragment was cloned into pMLBAD (25). The resulting plasmid was designated pMLBAD-BPSL1528 and introduced into *E. coli* DH5α, using $CaCl_2$-induced competent cells. pMLBAD-BPSL1528 was delivered into *B. pseudomallei* 25:90 by triparental mating using the donor strain *E. coli* DH5α(pMLBAD-BPSL1528), the recipient strain, and the helper strain *E. coli* Hb101(pRK2013) grown overnight in LB broth. One-hundred-microliter suspensions of the donor and helper strains were mixed directly together and incubated for 10 min at room temperature, followed by the addition of 200 μl of the recipient strain. This mixture was plated on Columbia agar plates for mating at 37°C for 4 h. The bacterial lawn of each plate was harvested using PBS, and aliquots were plated on trimethoprim- and tetracycline-containing plates for isolation of complemented Tn*5* mutants.

For mutant 54:55, the forward primer BF69 (5′-CCGGAATTCGCACATCT ACGAGACGATCTC-3′) and the reverse primer BF70 (5′-CCCAAGCTTAA CATGCTCGCGTTCGTCGTG-3′) (EcoRI and HindIII restriction sites are underlined) were used to amplify a 1,491-bp fragment from *B. pseudomallei* E8 genomic DNA containing the BPSL0395 coding region plus 573 bp upstream of the translational start and 432 bp downstream of the stop codon.

For mutant 56:65, the forward primer BF81 (5′-GCTCTAGAGCAGCGAA AACGGTGACGATT-3′) and the reverse primer BF82 (5′-CCCAAGCTTCTT TCGAGAACCTCTCGACGG-3′) (XbaI and HindIII restriction sites are underlined) were used to amplify a 1,218-bp fragment from *B. pseudomallei* E8 genomic DNA containing the BPSL2818 coding region plus 132 bp upstream of the translational start and 30 bp downstream of the stop codon.

For mutant 1:4, the forward primer BF87 (5′-CCGGAATTCCACAGCCCG CAGAGCAAGAGC-3′) and the reverse primer BF88 (5′-CCCAAGCTTGAG CATTCGTTCTGACGGCAC-3′) (EcoRI and HindIII restriction sites are underlined) were used to amplify a 2,292-bp fragment from *B. pseudomallei* E8 genomic DNA containing the BPSL2825 coding region plus 75 bp upstream of the translational start and 198 bp downstream of the stop codon.

Iron supplementation assay. Bacteria grown overnight in LB broth were washed repeatedly with 0.9% (wt/vol) NaCl, and 100 μl containing approximately 3×10^7 to 6×10^7 bacteria was plated on iron-depleted Vogel-Bonner agar (80 μM 2,2-dipyridyl as a chelator for free iron and 1.5% [wt/vol] agar [Difco high grade]). Sterile filter paper disks were placed on the agar, and 8 μl of Fe^{2+} (200 mM ferrous sulfate; Sigma) or hemin (10 mM; Sigma) was spotted on the disks.

TABLE 1. Phenotypic characteristics of *B. pseudomallei* mutants used in this study[d]

Chromosome	Strain	Gene[a]	Putative function, homology[a]	Plaque formation	Protease activity	Lecithinase activity	Siderophore production	Growth on supplemented iron-depleted agar		H_2O_2 resistance	Growth in LB medium	Growth in minimal medium
								Fe^{2+}	Hemin			
1	54:55	BPSL0395	Cytidylyltransferase	↓	+	+	−	+	+	+	+	+
	57:16	BPSL0413	Lipoate-protein ligase B, *lipB*	↓	+	+	+	+	−	↓	+	+
	30:93	BPSL0908	Phosphoribosylglycinamide formyltransferase, *purN*	↓	+	+	+	+	+	+	+	→
	25:90	BPSL1528	Putative exported protein	−	+	+	+	+	+	+	+	+
	56:65	BPSL2818[b]	Phosphoribosylformyl-glycinamidine cyclo-ligase, *purM*	↓	−	+	NG	NG	NG	ND	↓	−
	1:4	BPSL2825[c]	Para-aminobenzoate synthetase component, *pabB*	−	+	+	+	+	−	+	+	↓
	49:57	BPSL3133	Imidazole glycerol phosphate synthase, *hisF*	↓	+	+	+	NG	NG	+	+	−
2	5:45	BPSS1509	Hypothetical protein	↓	+	+	+	+	+	+	+	+
	16:48	BPSS1539	Hypothetical protein	↓	+	+	+	+	+	+	+	+

[a] Gene numbers, probable functions, and homologies are from reference 18.
[b] One of two isolated mutants with insertions in the same ORF at different positions.
[c] One of three isolated mutants with insertions in the same ORF at different positions.
[d] Plaque formation, production of extracellular enzymes, growth on iron-depleted medium supplemented with various iron sources, and H_2O_2 resistance were determined as described in Materials and Methods. +, wild-type plaque formation, enzyme activity, growth, or resistance; ↓, significant reduction; −, not detectable; NG, strain did not grow on medium; ND, not determined because growth was impaired under the assay conditions.

Plates were incubated at 37°C, and bacterial growth surrounding the disks was documented on days 6 and 7.

Siderophore and exoenzyme production. Siderophore and exoenzyme production was tested by streaking strains on appropriate indicator plates. Siderophore activity was measured using chromeazurol S agar (34). Siderophores remove iron from the chromeazurol S dye complex, resulting in a color change from blue to yellow halos around bacterial colonies. After 5 to 6 days, a yellow halo of ≥1 mm was considered a positive reaction. Since in *trans* complementation of mutants using pMLBAD resulted in impaired yellow halo formation per se, restoration of deficient siderophore production could not be tested after complementation of mutants. Proteolytic activity was determined on LB agar plates supplemented with 2% skim milk as described previously (19). Clear halos of >1 mm around bacterial colonies after incubation for 4 days indicated a positive reaction. The production of lecithinase was determined using egg yolk agar (Heipha, Eppelheim, Germany). After 48 h of incubation, white turbidity zones of ≥1 mm around bacterial colonies indicated enzyme activity.

H_2O_2 sensitivity assay. The H_2O_2 sensitivity disk assay was adapted from the work of Hassett et al. (16). Strains were grown overnight at 37°C in LB broth. One hundred microliters of culture containing approximately 2×10^7 to 5×10^7 bacteria was suspended in 3 ml of LB soft agar (0.6% [wt/vol] agar), mixed well, and poured on LB agar plates (with 1.5% [wt/vol] agar). Sterile filter paper disks were placed on the solid soft agar, and 8 μl of 30% (wt/vol) H_2O_2 was spotted onto the disks. Plates were incubated at 37°C for 24 h, and the diameters of zones of growth inhibition around the disks were measured. The experiments were done four times. The mean diameter of growth inhibition with the wild type was 4.0 cm (range, 3.8 to 4.3 cm in four experiments). The mean diameter of growth inhibition of the more sensitive 57:16 mutant was 4.7 cm (range, 4.3 to 4.9 cm), with an increase in diameter of ≥0.5 cm for the mutant compared to the wild type in each assay.

Swimming motility. Bacteria were grown on Columbia agar plates (Becton Dickinson) overnight and inoculated onto swimming LB agar plates containing 0.3% agar by the use of a sterile toothpick. Motility was assayed after 24 h of incubation at 37°C by determining the radius of the circular expansion pattern of bacterial migration from the point of inoculation.

Bacterial invasion and growth kinetics in HeLa cells. Twenty hours prior to infection, cells were seeded in 48-well plates containing 8×10^4 HeLa cells per well. Bacteria were grown in LB broth for 16 to 18 h and diluted in the respective cell culture medium to a multiplicity of infection (MOI) of 4. To infect HeLa cells, bacteria were centrifuged onto cells at 200 × *g* for 5 min at room temperature. After incubation at 37°C for 1 h, cells were washed twice with PBS and incubated with the respective cell culture medium containing 250 μg kanamycin per ml. This point was taken as time zero, and cells were further incubated for 1 h, 6 h, and 16 h to determine intracellular CFU. At these time points, cells were washed twice with PBS and subsequently lysed using 150 μl PBS containing 0.5% Tergitol (Fluka, Buchs, Switzerland) and 1% bovine serum albumin (BSA) per well. After 20 min of incubation, appropriate dilutions of these suspensions were plated on Ashdown agar and incubated at 37°C for 48 h, and colony counts were determined.

Invasion and growth kinetics in J774A.1 cells. Infection experiments with J774A.1 cells were performed as described for HeLa cells, with minor modifications. J774A.1 cells were seeded at 1.2×10^5 cells per well and infected at an MOI of 3:1. Bacteria were not centrifuged onto the cells for infection.

Immunofluorescence. Indirect immunofluorescence was performed essentially as previously described (4). Briefly, 1×10^5 Ptk2 cells were seeded on 12-mm glass coverslips in 24-well plates 18 to 20 h prior to infection. Bacteria were centrifuged onto cells at 1,650 × *g* for 15 min at room temperature at an MOI of 50:1. After incubation for 1 h at 37°C, the medium was exchanged for medium containing 250 μl kanamycin per ml and further incubated for 5 h after infection. Cells were washed twice with PBS and fixed with 4% paraformaldehyde in PBS at 4°C, followed by extraction for 1 min with 0.1% Triton X-100. Nonspecific binding sites were blocked for 30 min with 1% BSA. F actin was detected by using a 1:100 dilution of tetramethyl rhodamine isocyanate-phalloidin (Molecular Probes). For staining of lysosome-associated membrane glycoprotein 1 (LAMP-1), a mouse anti-human monoclonal antibody (clone H4A3; Pharmingen) was used at a 1:200 dilution. For staining of *B. pseudomallei*, we used either a murine monoclonal immunoglobulin G2b (IgG2b) isotype-switch variant of clone IgG1 3015 (36) or clone 3165 IgM (I. Steinmetz, unpublished data), both of which are reactive with a *B. pseudomallei* exopolysaccharide. As a secondary reagent, a 1:100 dilution of Alexa fluor 488-coupled goat anti-mouse antibody was used.

Murine infection model. Female 8- to 12-week-old BALB/c mice were obtained from Charles River Wiga (Sulzfeld, Germany). Animals were maintained under specific-pathogen-free conditions and were provided with food

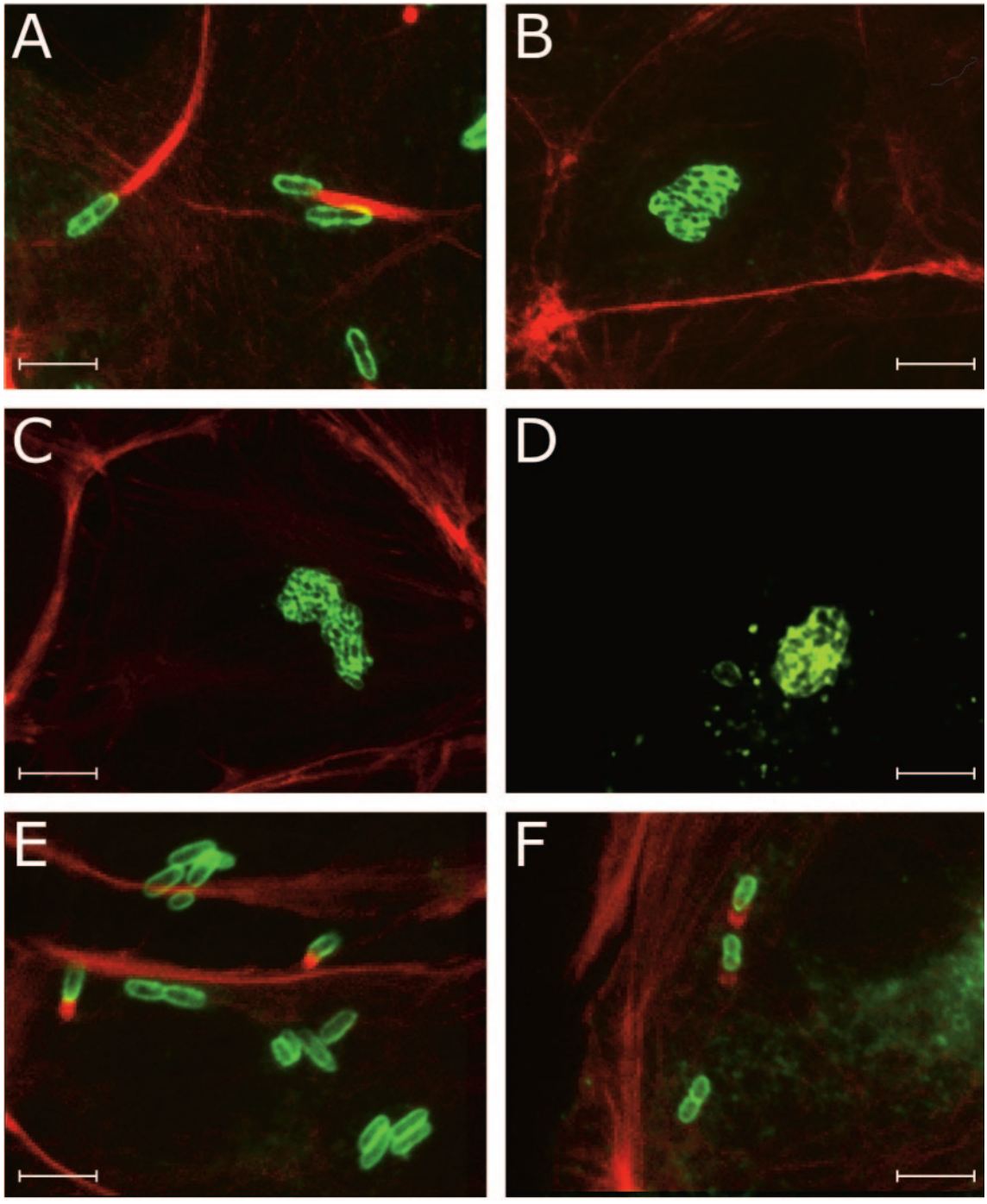

FIG. 1. Immunofluorescence microscopy of Ptk2 cells 6 h after infection with wild-type *B. pseudomallei* E8, mutant 16:48, or mutant 25:90. Infected HeLa cells were either double stained with antibodies to the bacteria (green) and with phalloidin for actin labeling (red) (A, B, C, E, and F) or stained with anti-LAMP-1 (green) (D). (A) Wild-type E8 reached the cytosol and induced actin tails. (B and C) Mutant 16:48 did not gain access to the cytosol but replicated in vacuoles and did not induce actin tails. (D) Mutant 16:48 cells containing vacuoles were shown to be LAMP-1 positive. (E and F) Mutant 25:90 formed only rudimentary actin tails. Bars, 5 μm in panels A, E, and F and 50 μm in panels B, C, and D.

and water ad libitum. For intranasal infection, mice were anesthetized with a mixture of ketamine hydrochloride and xylazine hydrochloride. Bacterial cells were grown for 18 to 20 h in LB broth and diluted in PBS to the required concentration, and 30 μl of this suspension was inoculated per animal into both nostrils. The mortality of animals was monitored daily, and survival curves were compared by using the log-rank test (GraphPad Prism, version 4.0). To enumerate bacteria in the spleen, liver, and lungs, the organs were aseptically removed and homogenized in 0.5 to 1 ml sterile PBS containing 0.5% Tergitol and 1% BSA, and the numbers of CFU were determined. The detection limit of this procedure was 5 to 15 CFU per organ, depending on the organ weight. In order to grow bacteria below this detection limit, all of the remaining homogenized organs were completely transferred to 5 ml LB broth and incubated for 48 h. One hundred microliters of this organ suspension was then plated purely on Ashdown agar to confirm that the organs were

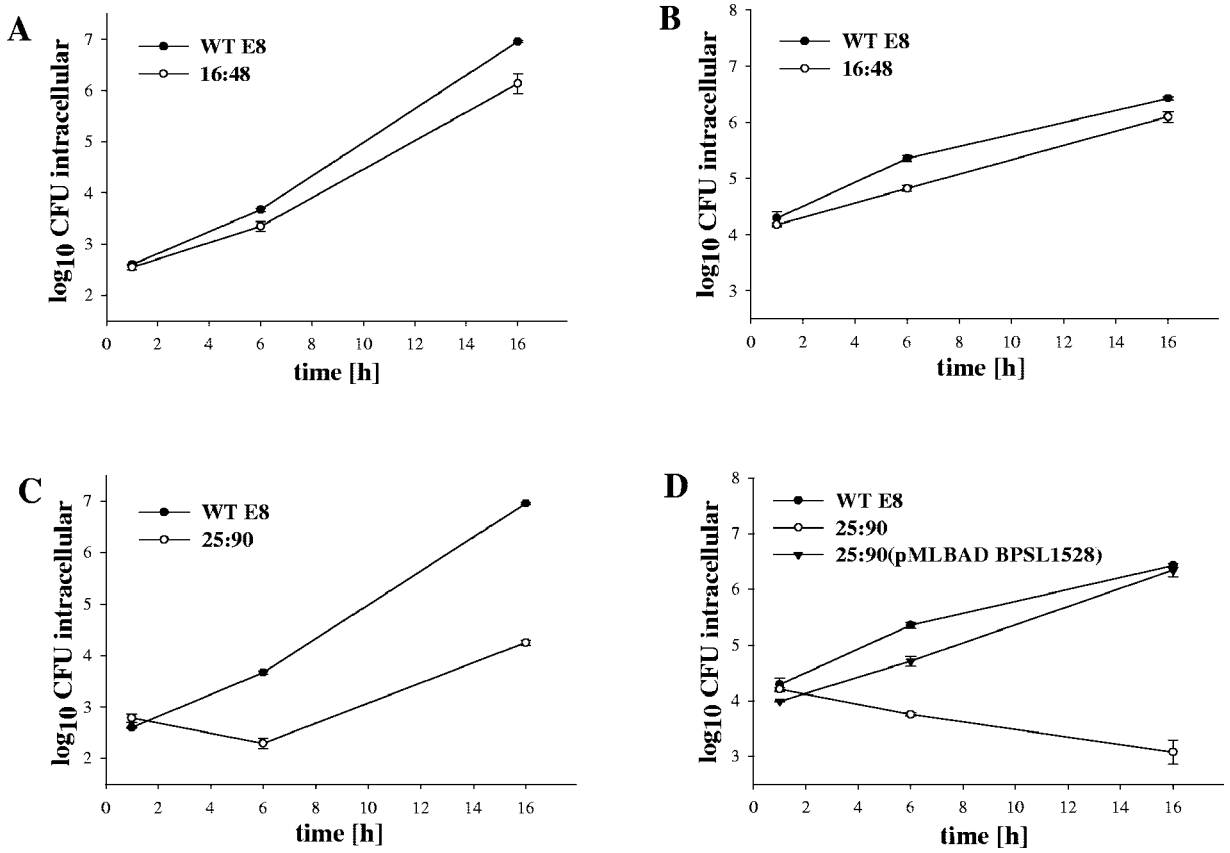

FIG. 2. Intracellular growth of mutants 16:48 and 25:90, complemented mutant 25:90, and *B. pseudomallei* E8 wild type in HeLa cells (A, C) and J774 A.1 macrophages (B, D). Values are the means ± standard deviations (SD) of triplicate determinations in single representative experiments. Similar results were obtained in at least three independent experiments with each bacterial strain.

sterile. Differences in bacterial loads were analyzed by using either a *t* test or the Mann-Whitney test (GraphPad Prism, version 4.0).

RESULTS AND DISCUSSION

Screening of *B. pseudomallei* transposon mutants for defects in intercellular spreading. We hypothesized that screening *B. pseudomallei* mutants for a reduced cell-to-cell spreading capacity on cell monolayers should reveal *B. pseudomallei* factors important at different stages of the intracellular life cycle. Approximately 6,000 transposon mutants were screened for a reduced ability to form plaques on PtK2 cell monolayers as a result of reduced intercellular spreading. For 12 mutants exhibiting either delayed or no plaque formation, the transposon insertion site was determined by a self-cloning procedure as described previously (11). DNA sequences were analyzed on the basis of the recently annotated *B. pseudomallei* genome (18). In two open reading frames (ORFs), the transposon inserted twice and three times (BPSL2818 and BPSL2825, respectively), at different positions. Table 1 shows the nine mutants with insertions in unrelated ORFs which were chosen for further characterization in this study. Southern blot analysis showed that each mutant contained only a single transposon insertion in the genome (data not shown).

Inactivation of gene BPSS1539 results in intracellular vacuole confinement and attenuated virulence. In mutant 16:48, which exhibited delayed plaque formation, the transposon disrupted BPSS1539, encoding a hypothetical protein within the Bsa type III secretion system gene cluster. Immunofluorescence microscopy revealed that mutant 16:48 was unable to escape from endocytic vesicles 6 h after infection (Fig. 1B and C). However, this mutant was still able to multiply intracellularly within the vacuoles, leading to large vesicles packed with bacteria. These vacuoles were never observed after wild-type infection and were shown to be positive for the lysosomal marker LAMP-1 (Fig. 1D), indicating that fusion with the late endosomal pathway had taken place. As a result of bacteria being trapped within the vacuoles, no actin tail formation could be detected at this time point (Fig. 1B and C). However, 12 h after infection, these huge vacuoles seemed to become leaky, and cytosolic cells of *B. pseudomallei* 16:48 were seen to be associated with actin tails (not shown), indicating that the induction of actin polymerization per se is retained in this mutant. Intracellular growth was confirmed when the intracellular CFU were determined for HeLa cells (Fig. 2A) as well as J774A.1 macrophages (Fig. 2B). The infection experiments with HeLa cells also demonstrated that mutant 16:48 had no invasion defect. A recently described *B. pseudomallei bipD* mutant lacking a component of the Bsa translocation apparatus was also unable to escape from vacuoles, but in addition, in contrast to mutant 16:48, was found to be severely impaired in intracellu-

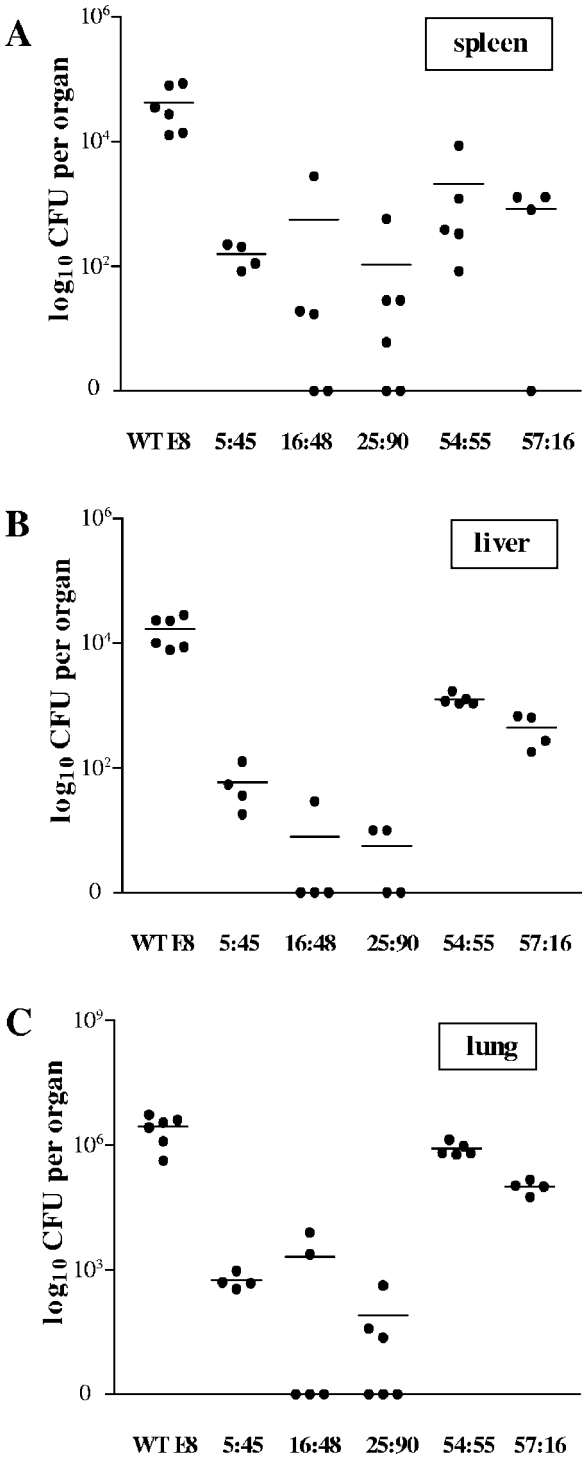

FIG. 3. Determination of bacterial burdens in spleen (A), liver (B), and lungs (C) after intranasal infection with ~2×10^2 CFU of either *B. pseudomallei* WT E8 or mutants. Single dots represent CFU in the respective organs from single animals. The horizontal lines represent the means. Bacterial counts of all mutants were significantly lower in all three organs compared to those of the wild type ($P < 0.05$).

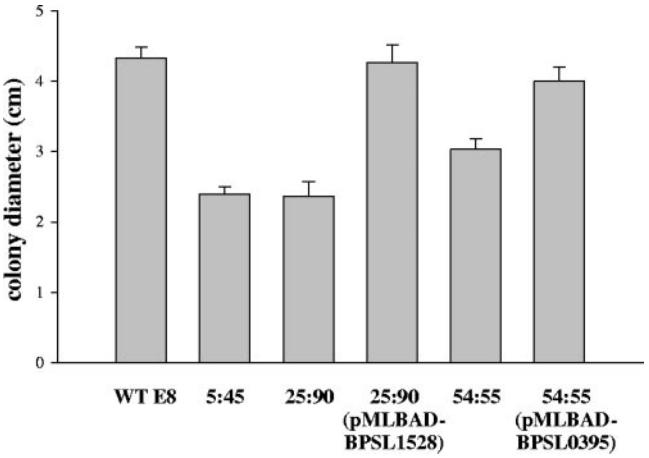

FIG. 4. Swimming motility of mutants 25:90, 54:55, and 5:45 and the complemented mutants 25:90(pMLBAD-BPSL1528) and 54:55(pMLBAD-BPSL0395) compared to that of the wild type. Motility was assayed after 24 h of incubation at 37°C by determining the diameter of circular bacterial migration from the point of inoculation. Values are the mean diameters ± SD from triplicate values of a representative experiment.

lar survival (41), indicating that multiple effectors are probably affected in the *bipD* mutant.

To assess the role of BPSS1539 inactivation on in vivo virulence, BALB/c mice were intranasally infected with mutant 16:48. In this model, the 50% lethal dose (LD_{50}) of the WT strain E8 at 4 weeks postinfection is <10 CFU. Mutant strain 16:48 revealed a significantly reduced mortality ($P = 0.0005$ versus WT E8) during the observation period after challenge with 2×10^2 CFU (see Fig. 7A), although the degree of attenuation was the least pronounced compared to the other mutants identified in this study (see below). However, mutant 16:48 also resulted in a decreased bacterial burden at 48 h postchallenge in the spleen, liver, and lungs (Fig. 3). Since we did not test a complemented 16:48 mutant, we cannot formally exclude the possibility that a polar or second-site effect caused the observed virulence defect. In a recent study, mutations of the Bsa translocator protein BipD were shown to result in a significant delay in the time to death for BALB/c mice following intranasal infection and also in a reduced bacterial burden in the early

TABLE 2. In vivo attenuation of *B. pseudomallei* mutants in a BALB/c model of intranasal infection

Strain	LD_{50} range[a]
E8 WT	<10
16:48	≈2×10^2
54:55	>2×10^2–<5×10^3
57:16	>2×10^2–<5×10^3
5:45	>5×10^3–<10^7
49:57	>5×10^3–<10^7
30:93	>10^6–<10^7
1:4	>10^7
56:65	>10^7
25:90	>10^7

[a] Values are CFU inferred from the data shown in Fig. 7 and data presented in the text.

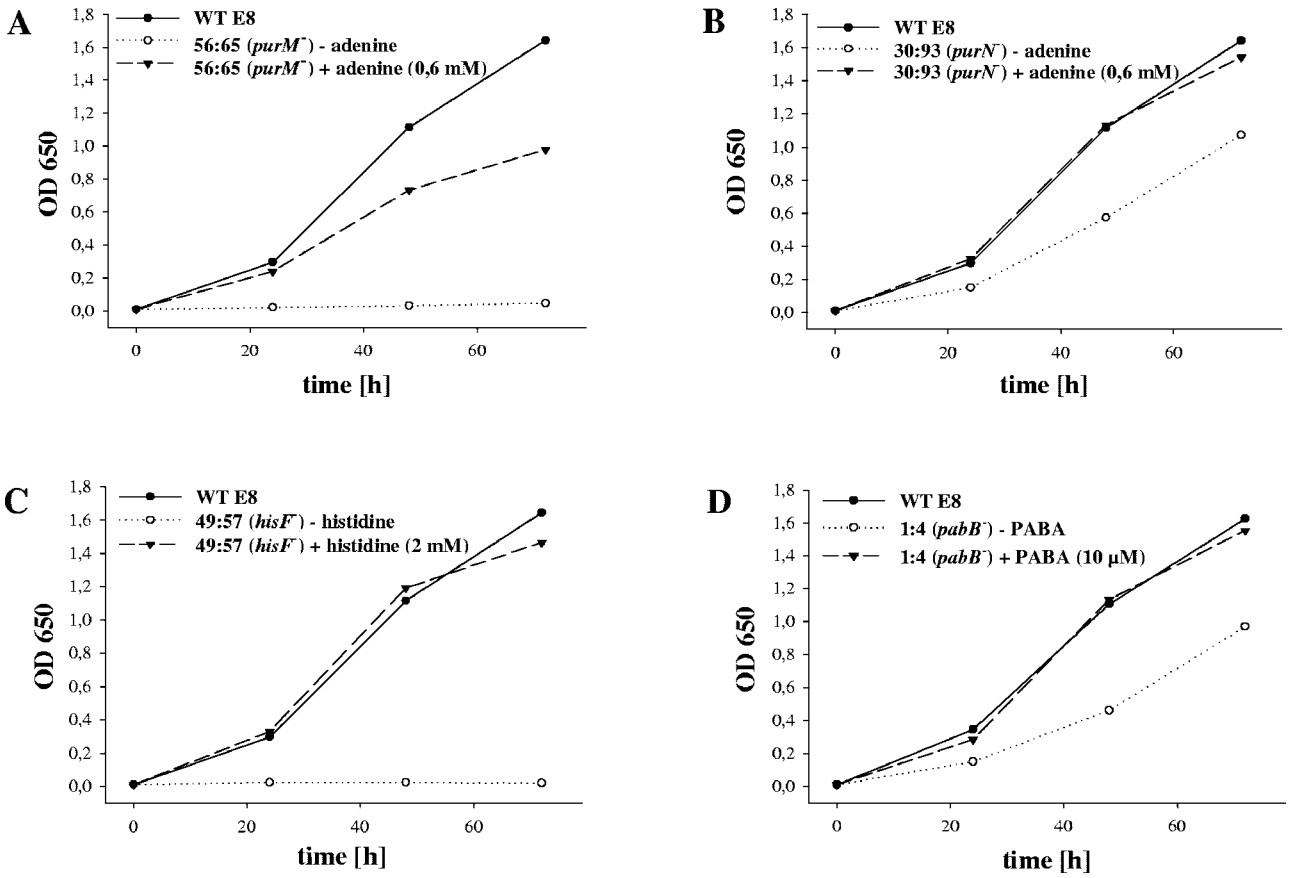

FIG. 5. Growth kinetics of *B. pseudomallei* mutants 56:65 (A), 30:93 (B), 49:57 (C), and 1:4 (D) in Vogel-Bonner minimal medium with and without respective supplementation. Data for one of three experiments with similar results are shown.

phase of infection (39). Mutants of the putative effectors BopA and BopB were only slightly attenuated compared to the *bipD* mutant (39). *B. pseudomallei* mutants lacking the known type III secreted effector BobE were not attenuated. The phenotype of *B. pseudomallei* 16:48 is clearly different from that of *Listeria monocytogenes* mutants defective in production of listeriolysin O, the effector molecule responsible for vacuolar lysis of this bacterium. Listeriolysin O-negative mutants are also retained within vacuoles but are not able to multiply intracellularly and are avirulent in mice (14, 42).

Inactivation of gene BPSL1528 leads to impaired actin tail formation, reduced intracellular survival, and high-grade attenuation of virulence. In mutant strain 25:90, which exhibited no plaque formation, the transposon disrupted BPSL1528, encoding a putative exported protein. Immunofluorescence microscopy of mutant 25:90 revealed severely impaired actin tail formation, resulting in only rudimentary actin tails (Fig. 1E and F). The formation of protrusions could not be detected. Moreover, intracellular growth was severely restricted in HeLa cells compared to that of the wild type, although invasion was not impaired (Fig. 2C). In J774A.1 macrophages, bacterial numbers of mutant 25:90 decreased over time (Fig. 2D), whereas extracellular growth in either LB or minimal medium was not affected (Table 1). Furthermore, mutant 25:90 revealed reduced swimming motility (Fig. 4). Complementation in *trans* of BPSL1528 restored intracellular growth in macrophages (Fig. 2D) as well as swimming motility (Fig. 4), indicating that the mutation of BPSL1528, rather than polar or second-site mutations, caused the observed phenotype. Intranasal infection of BALB/c mice with mutant 25:90 revealed high-grade attenuation (Table 2; see Fig. 7C). All animals challenged with 10^7 CFU survived and showed no signs of clinical illness. The mutant strain 25:90 also exhibited significantly lower bacterial burdens in the spleen, liver, and lungs 48 h after infection (Fig. 3). The *trans*-complemented mutant 25:90 also had restored in vivo virulence ($P = 0.0012$ versus mutant 25:90) (see Fig. 7D). The pleiotropic phenotype of the defect in BPSL1528 argues for a regulatory function of the encoded protein on various virulence factors rather than a single effector molecule.

Inactivation of a putative lipoate-protein ligase B (LipB) (BPSL0413), a hypothetical protein (BPSS1509), and a putative cytidylyltransferase (BPSL0395) results in attenuated virulence. Mutants 57:16, 5:45, and 54:55 showed delayed plaque formation, and genetic analysis revealed the insertion of the transposon in a gene for a putative lipoate-protein ligase B (*lipB*) (BPSL0413), a gene for a hypothetical protein (BPSS1509), and an intergenic region 95 bp upstream of the predicted translation initiation codon of BPSL0395, encoding a putative cytidylyltransferase (Table 1). Immunofluorescence microscopy of these mutants showed that the formation of actin tails and

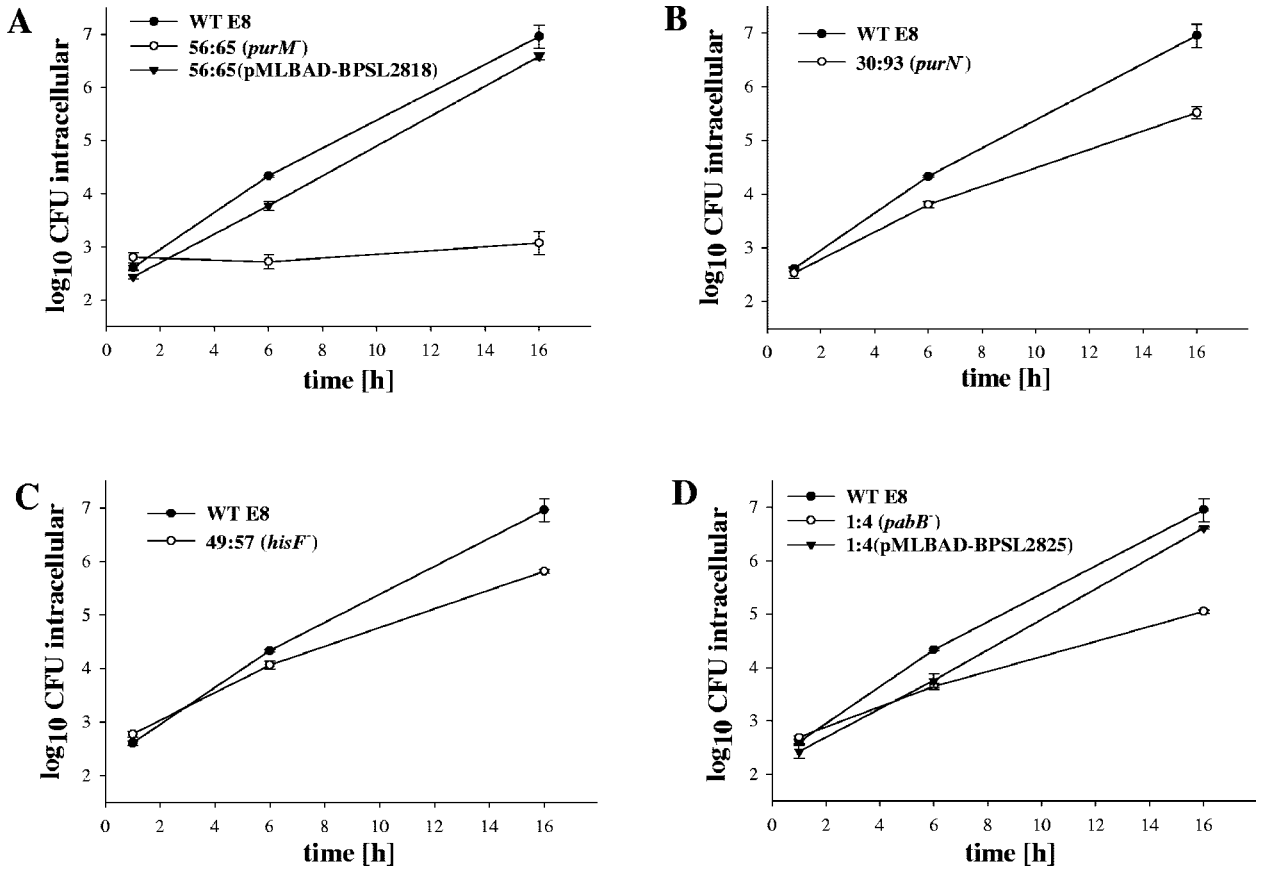

FIG. 6. Intracellular growth of mutants 56:65 (A), 30:93 (B), 49:57 (C), and 1:4 (D), complemented mutants, and *B. pseudomallei* WT E8 in HeLa cells. Values are the means ± SD of triplicate determinations for a representative experiment. Similar results were obtained in at least three independent experiments with each bacterial strain.

protrusions was unaffected (not shown). Furthermore, we could not detect an intracellular growth defect in HeLa cells and J774A.1 macrophages (data not shown). With respect to the reduced plaque-forming capacities of these mutants, one might speculate that the intracellular growth experiments performed with these cell lines were not sensitive enough to detect only a slight reduction in intracellular survival or growth compared to the plaque assay based on Ptk2 cells. Alternatively, these mutants might have other defects in the progression of the intracellular life cycle leading to the reduced intercellular spreading capacity observed in the plaque assay. Further characterization of mutants 5:45, 54:55, and 57:16 with respect to swimming motility, iron acquisition, and oxidative stress revealed some deviations relative to the wild type (Table 1 and Fig. 4). Strain 57:16 did not grow under iron-depleted conditions with hemin supplementation but did grow with Fe^{2+} repletion. In addition, mutant 57:16 revealed a higher susceptibility to H_2O_2. Mutant 5:45 revealed reduced swimming motility (Fig. 4). Swimming motility was also reduced in mutant 54:55. *Trans*-complementation of BPSL0395 in mutant 54:55 restored swimming motility (Fig. 4), providing evidence that the BPSL0395 mutation was responsible for the observed phenotype. In mutant 54:55, no siderophore production could be detected. The restoration of siderophore production in the complemented mutant 54:55 could not be tested (see Materials and Methods for details). In contrast to the case with the wild type, no animals died at 4 weeks after intranasal infection of BALB/c mice with 2×10^2 CFU of either mutant 57:16 ($n = 4$; $P = 0.0047$ versus WT E8), mutant 5:45 ($n = 4$; $P = 0.0047$ versus WT E8), or mutant 54:55 ($n = 5$; $P = 0.0016$ versus WT E8), indicating significant roles of BPSL0413, BPSS1509, and BPSL0395 in the pathogenesis of infection. However, when mice were challenged with 5×10^3 CFU, no animals survived infection with mutant 54:55, in contrast to infections with mutants 5:45 and 57:16 (Table 2; see Fig. 7B) ($P = 0.0035$ for 54:55 versus 5:45; $P = 0.0279$ for 54:55 versus 57:16), indicating a higher level of attenuation of the last two strains. The reduced mortality of all three mutants correlated with reduced bacterial burdens at 48 h postinfection (Fig. 3). The pleiotropic effects of BPSS1509 on motility, of BPSL0395 on iron acquisition and motility, and of BPSL0413 on iron acquisition and oxidative stress might be indicative of regulatory functions of these genes. A possible role of lipoyl modifications of proteins, and thus of a lipoate-protein ligase, for in vivo replication of *B. pseudomallei*, as indicated by the *lipB* (BPSL0413) mutant, is consistent with a recent study showing that a lipoate-protein ligase (LplA1) of *Listeria monocytogenes* is important for growth in the host cytosol and for virulence in mice (28).

Inactivation of *B. pseudomallei* purine (BPSL0908 and BPSL2818), histidine (BPSL3133), and *para*-aminobenzoate

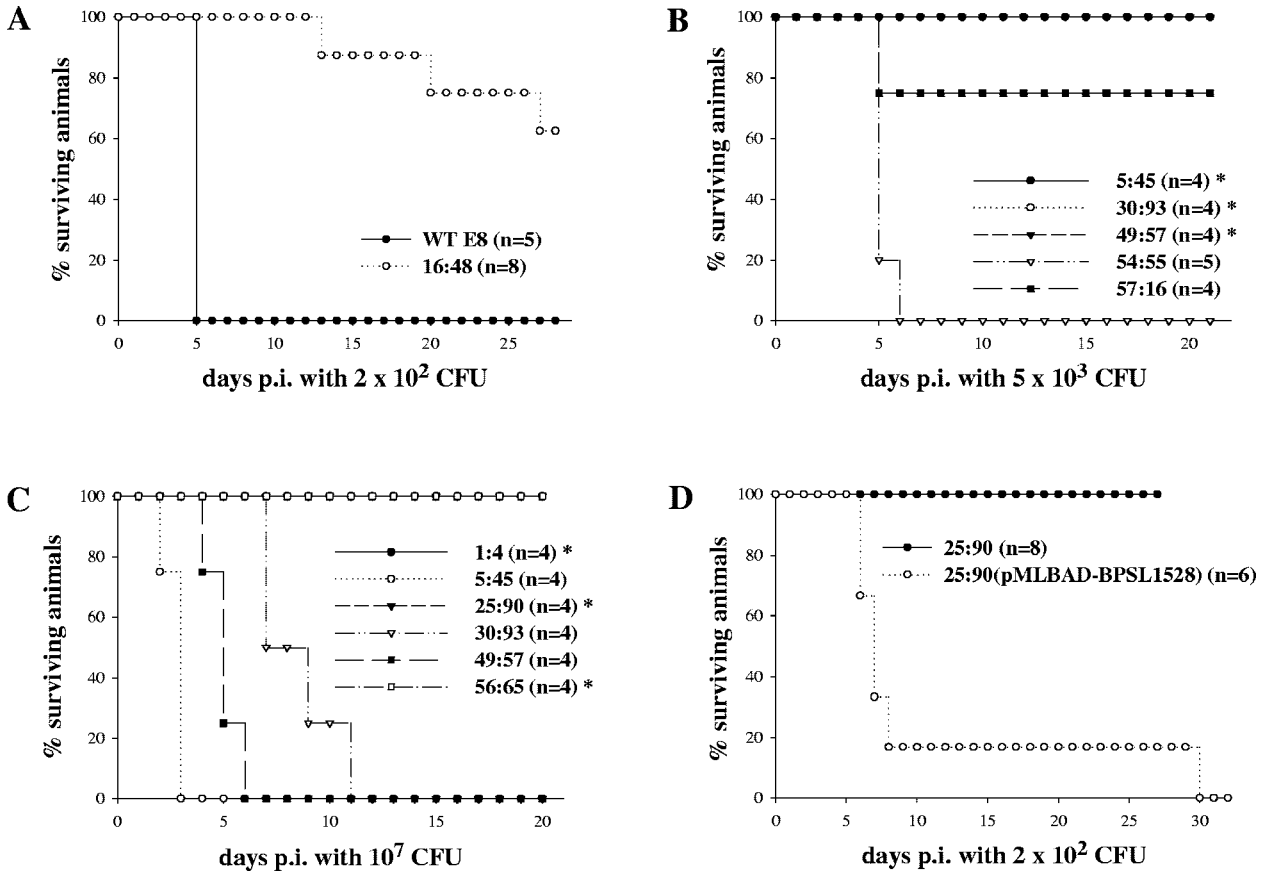

FIG. 7. Survival of BALB/c mice after intranasal infection with *B. pseudomallei* WT E8 and plaque assay mutants. (A) Infection with ~2×10^2 CFU of *B. pseudomallei* WT E8 and mutant 16:48. (B) Infection with ~5×10^3 CFU of mutants 5:45, 30:93, 49:57, 54:55, and 57:16. (C) Infection with ~10^7 CFU of mutants 1:4, 5:45, 25:90, 30:93, 49:57, and 56:65. (D) Infection with ~2×10^2 CFU of mutant 25:90 and its complemented mutant. *, all animals infected with these mutants survived for the observed time period.

(BPSL2825) biosynthetic pathway genes results in intracellular growth defects and attenuated virulence. A group of four mutants with defects in putative *B. pseudomallei* biosynthetic enzymes revealed either reduced or no growth in minimal medium (Table 1). To obtain biochemical evidence for the defects in the various putative biosynthetic pathways, we performed supplementation experiments in minimal medium (Fig. 5). Mutant 56:65, with delayed plaque formation and a defect in the BPSL2818 gene (*purM*), encoding a putative phosphoribosylformyl-glycinamidine cyclo-ligase, did not grow in minimal medium, and no protease activity could be detected (Table 1). This mutant is a purine auxotroph since supplementation with adenine restored growth (Fig. 5A). In contrast, mutant 30:93, with a defect in the BPSL0908 gene (*purN*), encoding a putative phosphoribosylglycinamide formyltransferase, showed only reduced growth. This growth defect could be restored to the wild-type level by adding adenine (Fig. 5B). For both mutants, the addition of pyrimidines had no effect on growth (not shown). In order to test the hypothesis that the reduced plaque-forming capacities of these purine biosynthesis pathway mutants are due to an intracellular growth defect, HeLa cells were infected, and intracellular CFU were determined at different time points. Experiments showed impaired growth for the *purN* mutant 30:93 compared to the wild type (Fig. 6B), whereas the *purM* mutant 56:65 showed no intracellular replication during the experiment (Fig. 6A). *Trans*-complementation of the *purM* mutant 56:65 restored growth on minimal medium agar, protease activity, and intracellular growth (Fig. 6A), with the last parameter indicating a crucial role of BPSL2818 in the intracellular habitat of *B. pseudomallei*. Neither the *purM* nor the *purN* mutant was defective in cellular invasion compared to the wild type (Fig. 6A and B). Moreover, immunofluorescence microscopy revealed that these mutants were able to induce the formation of actin tails and protrusions (not shown). It seems possible that the less severe phenotype of the *purN* mutant 30:93 is due to an intact *purT* homologue in *B. pseudomallei* (BPSL1111), which might also be capable of catalyzing the third step in the purine biosynthetic pathway, as shown in *Escherichia coli* (27), thereby resulting in a rather mild growth defect relative to that of the *purM* mutant 56:65, where obviously no alternative pathway exists.

Mutations in the purine biosynthetic pathway have previously been shown to reduce virulence in different bacterial pathogens (7, 21, 29). Indeed, some decades ago, a genetically undefined *B. pseudomallei* purine auxotroph was shown to be attenuated (26) in mice. Both the *purN* and *purM* mutants were significantly attenuated in BALB/c mice (Fig. 7B and C and Table 2). In accordance with the in vitro results, the attenua-

tion of mutant 56:65 was more pronounced than that of mutant 30:93. After challenge of mice with 10^7 CFU of mutant 56:65, all animals survived and showed no clinical signs of illness, whereas mice did not survive this infectious dose with mutant 30:93 ($P = 0.0062$ for 30:93 versus 56:65) (Fig. 7C). However, all animals ($n = 4$) survived an infectious dose of 10^6 CFU with mutant 30:93.

Analysis of mutant 49:57, which showed delayed plaque formation, revealed a defect in BPSL3133 (*hisF*), encoding a putative imidazole glycerol phosphate synthase. This mutant was shown to be a histidine auxotroph, which grew as well as the wild type when histidine was added to the minimal medium (Fig. 5C). Neither the addition of other amino acids, such as phenylalanine or glutamine, nor the addition of purines and pyrimidines restored the growth of mutant 49:57 (not shown). The fact that mutant 49:57 showed intracellular growth, although it was impaired (Fig. 6C), makes it likely that some intracellular supplementation with histidine occurred under the experimental conditions applied. Neither the invasion of mutant 49:57 into HeLa cells (Fig. 6C) nor the formation of actin tails and protrusions (not shown) was affected. Intranasal infection of BALB/c mice with mutant 49:57 revealed a significant attenuation, since all mice survived a challenge with 5×10^3 CFU ($P = 0.0035$ for 49:57 versus 54:55) (Fig. 7B and Table 2), indicating that the histidine supply in vivo was not sufficient to completely restore virulence. However, all animals died after infection with 10^7 CFU of mutant 49:57 (Fig. 7C).

The impaired growth of the non-plaque-forming mutant 1:4, with a defect in BPSL2825 (*pabB*), encoding a putative *para*-aminobenzoate synthetase component, in minimal medium could be supplemented to the wild-type level by adding PABA (Fig. 5D), whereas the addition of, e.g., histidine had no effect. Figure 5D shows that mutant 1:4 entered HeLa cells to the same extent as the wild type but exhibited reduced intracellular growth. The formation of actin tails and cell protrusions was not affected (not shown). *Trans*-complementation could restore the growth of mutant 1:4 to the wild-type level (Fig. 6D), verifying the importance of BPSL2825 in the intracellular habitat. Further experiments revealed an effect of BPSL2825 on iron acquisition, since mutant 1:4 could not grow on iron-depleted agar with hemin as the sole iron source, in contrast to the wild type, whereas the utilization of Fe^{2+} was not affected (Table 1). Complementation of mutant 1:4 restored the ability to use hemin as the sole iron source. In contrast to the relatively moderate intracellular growth defect observed in vitro, a challenge of BALB/c mice with mutant 1:4 revealed high-grade attenuation. All animals challenged intranasally with 10^7 CFU not only survived ($P = 0.0062$ for 1:4 versus 30:93) (Fig. 7C and Table 2) but showed no signs of clinical illness, indicating an important role of BPSL2825 in virulence.

Our experiments suggest that components of the *B. pseudomallei* purine, PABA, and histidine biosynthesis pathways are limited in the intracellular habitat and therefore that mutations in these pathways impair intracellular multiplication of *B. pseudomallei*. The genes involved are also important for in vivo virulence, although their in vivo importance varies greatly. In addition, an effect of BPSL2825 (*pabB*) on hemin utilization as an iron source might play an important role in the decreased intracellular fitness and profound virulence attenuation in vivo. Attenuated mutants of a number of intracellular pathogens have been investigated as live vaccine candidates for the induction of protective immunity (15, 17). A recently described *B. pseudomallei* mutant which is auxotrophic in the branched-chain-amino-acid biosynthetic pathway conferred protection against wild-type challenge in BALB/c mice (2), although data on the intracellular behavior of this mutant were not provided. We are currently investigating the protective potential of the highly attenuated mutants with defects in various biosynthetic pathways isolated in this study.

In conclusion, the experimental approach described in this study led to the identification of a number of novel *B. pseudomallei* virulence determinants that are important for in vivo pathogenicity in a murine model of infection. Furthermore, we identified *B. pseudomallei* biosynthetic pathway genes which appear to be essential for intracellular growth. Finally, our results indicate that the intracellular life style of *B. pseudomallei* is important for causing disease.

REFERENCES

1. **Ashdown, L. R.** 1979. An improved screening technique for isolation of Pseudomonas pseudomallei from clinical specimens. Pathology **11:**293–297.
2. **Atkins, T., R. G. Prior, K. Mack, P. Russell, M. Nelson, P. C. Oyston, G. Dougan, and R. W. Titball.** 2002. A mutant of *Burkholderia pseudomallei*, auxotrophic in the branched chain amino acid biosynthetic pathway, is attenuated and protective in a murine model of melioidosis. Infect. Immun. **70:**5290–5294.
3. **Attree, O., and I. Attree.** 2001. A second type III secretion system in Burkholderia pseudomallei: who is the real culprit? Microbiology **147:**3197–3199.
4. **Breitbach, K., K. Rottner, S. Klocke, M. Rohde, A. Jenzora, J. Wehland, and I. Steinmetz.** 2003. Actin-based motility of Burkholderia pseudomallei involves the Arp 2/3 complex, but not N-WASP and Ena/VASP proteins. Cell. Microbiol. **5:**385–393.
5. **Chaowagul, W., N. J. White, D. A. Dance, Y. Wattanagoon, P. Naigowit, T. M. Davis, S. Looareesuwan, and N. Pitakwatchara.** 1989. Melioidosis: a major cause of community-acquired septicemia in northeastern Thailand. J. Infect. Dis. **159:**890–899.
6. **Choy, J. L., M. Mayo, A. Janmaat, and B. J. Currie.** 2000. Animal melioidosis in Australia. Acta Trop. **74:**153–158.
7. **Crawford, R. M., L. Van De Verg, L. Yuan, T. L. Hadfield, R. L. Warren, E. S. Drazek, H. H. Houng, C. Hammack, K. Sasala, T. Polsinelli, J. Thompson, and D. L. Hoover.** 1996. Deletion of *purE* attenuates *Brucella melitensis* infection in mice. Infect. Immun. **64:**2188–2192.
8. **Currie, B. J., D. A. Fisher, D. M. Howard, J. N. Burrow, D. Lo, S. Selva-Nayagam, N. M. Anstey, S. E. Huffam, P. L. Snelling, P. J. Marks, D. P. Stephens, G. D. Lum, S. P. Jacups, and V. L. Krause.** 2000. Endemic melioidosis in tropical northern Australia: a 10-year prospective study and review of the literature. Clin. Infect. Dis. **31:**981–986.
9. **Dance, D. A.** 2002. Melioidosis. Curr. Opin. Infect. Dis. **15:**127–132.
10. **Dance, D. A.** 1991. Pseudomonas pseudomallei: danger in the paddy fields. Trans. R. Soc. Trop. Med. Hyg. **85:**1–3.
11. **DeShazer, D., P. J. Brett, R. Carlyon, and D. E. Woods.** 1997. Mutagenesis of *Burkholderia pseudomallei* with Tn*5*-OT182: isolation of motility mutants and molecular characterization of the flagellin structural gene. J. Bacteriol. **179:**2116–2125.
12. **DeShazer, D., P. J. Brett, and D. E. Woods.** 1998. The type II O-antigenic polysaccharide moiety of Burkholderia pseudomallei lipopolysaccharide is required for serum resistance and virulence. Mol. Microbiol. **30:**1081–1100.
13. **Gan, Y. H., K. L. Chua, H. H. Chua, B. Liu, C. S. Hii, H. L. Chong, and P. Tan.** 2002. Characterization of Burkholderia pseudomallei infection and identification of novel virulence factors using a Caenorhabditis elegans host system. Mol. Microbiol. **44:**1185–1197.
14. **Gedde, M. M., D. E. Higgins, L. G. Tilney, and D. A. Portnoy.** 2000. Role of listeriolysin O in cell-to-cell spread of *Listeria monocytogenes*. Infect. Immun. **68:**999–1003.
15. **Handman, E.** 2001. Leishmaniasis: current status of vaccine development. Clin. Microbiol. Rev. **14:**229–243.
16. **Hassett, D. J., J. F. Ma, J. G. Elkins, T. R. McDermott, U. A. Ochsner, S. E. West, C. T. Huang, J. Fredericks, S. Burnett, P. S. Stewart, G. McFeters, L. Passador, and B. H. Iglewski.** 1999. Quorum sensing in Pseudomonas aeruginosa controls expression of catalase and superoxide dismutase genes and

mediates biofilm susceptibility to hydrogen peroxide. Mol. Microbiol. **34:** 1082–1093.
17. **Hingley-Wilson, S. M., V. K. Sambandamurthy, and W. R. Jacobs, Jr.** 2003. Survival perspectives from the world's most successful pathogen, Mycobacterium tuberculosis. Nat. Immunol. **4:**949–955.
18. **Holden, M. T., R. W. Titball, S. J. Peacock, A. M. Cerdeno-Tarraga, T. Atkins, L. C. Crossman, T. Pitt, C. Churcher, K. Mungall, S. D. Bentley, M. Sebaihia, N. R. Thomson, N. Bason, I. R. Beacham, K. Brooks, K. A. Brown, N. F. Brown, G. L. Challis, I. Cherevach, T. Chillingworth, A. Cronin, B. Crossett, P. Davis, D. DeShazer, T. Feltwell, A. Fraser, Z. Hance, H. Hauser, S. Holroyd, K. Jagels, K. E. Keith, M. Maddison, S. Moule, C. Price, M. A. Quail, E. Rabbinowitsch, K. Rutherford, M. Sanders, M. Simmonds, S. Songsivilai, K. Stevens, S. Tumapa, M. Vesaratchavest, S. Whitehead, C. Yeats, B. G. Barrell, P. C. Oyston, and J. Parkhill.** 2004. Genomic plasticity of the causative agent of melioidosis, Burkholderia pseudomallei. Proc. Natl. Acad. Sci. USA **101:**14240–14245.
19. **Huber, B., K. Riedel, M. Hentzer, A. Heydorn, A. Gotschlich, M. Givskov, S. Molin, and L. Eberl.** 2001. The cep quorum-sensing system of Burkholderia cepacia H111 controls biofilm formation and swarming motility. Microbiology **147:**2517–2528.
20. **Inglis, T. J., S. C. Garrow, C. Adams, M. Henderson, M. Mayo, and B. J. Currie.** 1999. Acute melioidosis outbreak in Western Australia. Epidemiol. Infect. **123:**437–443.
21. **Jackson, M., S. W. Phalen, M. Lagranderie, D. Ensergueix, P. Chavarot, G. Marchal, D. N. McMurray, B. Gicquel, and C. Guilhot.** 1999. Persistence and protective efficacy of a *Mycobacterium tuberculosis* auxotroph vaccine. Infect. Immun. **67:**2867–2873.
22. **Jones, A. L., T. J. Beveridge, and D. E. Woods.** 1996. Intracellular survival of *Burkholderia pseudomallei*. Infect. Immun. **64:**782–790.
23. **Kespichayawattana, W., S. Rattanachetkul, T. Wanun, P. Utaisincharoen, and S. Sirisinha.** 2000. *Burkholderia pseudomallei* induces cell fusion and actin-associated membrane protrusion: a possible mechanism for cell-to-cell spreading. Infect. Immun. **68:**5377–5384.
24. **Leelarasamee, A., and S. Bovornkitti.** 1989. Melioidosis: review and update. Rev. Infect. Dis. **11:**413–425.
25. **Lefebre, M. D., and M. A. Valvano.** 2002. Construction and evaluation of plasmid vectors optimized for constitutive and regulated gene expression in *Burkholderia cepacia* complex isolates. Appl. Environ. Microbiol. **68:**5956–5964.
26. **Levine, H. B., and R. L. Maurer.** 1958. Immunization with an induced avirulent auxotrophic mutant of Pseudomonas pseudomallei. J. Immunol. **81:**433–438.
27. **Nygaard, P., and J. M. Smith.** 1993. Evidence for a novel glycinamide ribonucleotide transformylase in *Escherichia coli*. J. Bacteriol. **175:**3591–3597.
28. **O'Riordan, M., M. A. Moors, and D. A. Portnoy.** 2003. Listeria intracellular growth and virulence require host-derived lipoic acid. Science **302:**462–464.
29. **Potvin, E., D. E. Lehoux, I. Kukavica-Ibrulj, K. L. Richard, F. Sanschagrin, G. W. Lau, and R. C. Levesque.** 2003. In vivo functional genomics of Pseudomonas aeruginosa for high-throughput screening of new virulence factors and antibacterial targets. Environ. Microbiol. **5:**1294–1308.
30. **Pruksachartvuthi, S., N. Aswapokee, and K. Thankerngpol.** 1990. Survival of Pseudomonas pseudomallei in human phagocytes. J. Med. Microbiol. **31:** 109–114.
31. **Rainbow, L., C. A. Hart, and C. Winstanley.** 2002. Distribution of type III secretion gene clusters in Burkholderia pseudomallei, B. thailandensis and B. mallei. J. Med. Microbiol. **51:**374–384.
32. **Reckseidler, S. L., D. DeShazer, P. A. Sokol, and D. E. Woods.** 2001. Detection of bacterial virulence genes by subtractive hybridization: identification of capsular polysaccharide of *Burkholderia pseudomallei* as a major virulence determinant. Infect. Immun. **69:**34–44.
33. **Rotz, L. D., and J. M. Hughes.** 2004. Advances in detecting and responding to threats from bioterrorism and emerging infectious disease. Nat. Med. **10:**S130–S136.
33a. **Sambrook, J., E. F. Fritsch, and T. Maniatis.** 1989. Molecular cloning: a laboratory manual, 2nd ed. Cold Spring Harbor Laboratory Press, Cold Spring Harbor, N.Y.
34. **Schwyn, B., and J. B. Neilands.** 1987. Universal chemical assay for the detection and determination of siderophores. Anal. Biochem. **160:**47–56.
35. **Song, Y., C. Xie, Y. M. Ong, Y. H. Gan, and K. L. Chua.** 2005. The BpsIR quorum-sensing system of *Burkholderia pseudomallei*. J. Bacteriol. **187:**785–790.
36. **Steinmetz, I., M. Rohde, and B. Brenneke.** 1995. Purification and characterization of an exopolysaccharide of *Burkholderia* (*Pseudomonas*) *pseudomallei*. Infect. Immun. **63:**3959–3965.
37. **Stevens, M. P., A. Friebel, L. A. Taylor, M. W. Wood, P. J. Brown, W. D. Hardt, and E. E. Galyov.** 2003. A *Burkholderia pseudomallei* type III secreted protein, BopE, facilitates bacterial invasion of epithelial cells and exhibits guanine nucleotide exchange factor activity. J. Bacteriol. **185:**4992–4996.
38. **Stevens, M. P., and E. E. Galyov.** 2004. Exploitation of host cells by Burkholderia pseudomallei. Int. J. Med. Microbiol. **293:**549–555.
39. **Stevens, M. P., A. Haque, T. Atkins, J. Hill, M. W. Wood, A. Easton, M. Nelson, C. Underwood-Fowler, R. W. Titball, G. J. Bancroft, and E. E. Galyov.** 2004. Attenuated virulence and protective efficacy of a Burkholderia pseudomallei bsa type III secretion mutant in murine models of melioidosis. Microbiology **150:**2669–2676.
40. **Stevens, M. P., J. M. Stevens, R. L. Jeng, L. A. Taylor, M. W. Wood, P. Hawes, P. Monaghan, M. D. Welch, and E. E. Galyov.** 2005. Identification of a bacterial factor required for actin-based motility of Burkholderia pseudomallei. Mol. Microbiol. **56:**40–53.
41. **Stevens, M. P., M. W. Wood, L. A. Taylor, P. Monaghan, P. Hawes, P. W. Jones, T. S. Wallis, and E. E. Galyov.** 2002. An Inv/Mxi-Spa-like type III protein secretion system in Burkholderia pseudomallei modulates intracellular behaviour of the pathogen. Mol. Microbiol. **46:**649–659.
42. **Tilney, L. G., and D. A. Portnoy.** 1989. Actin filaments and the growth, movement, and spread of the intracellular bacterial parasite, Listeria monocytogenes. J. Cell Biol. **109:**1597–1608.
43. **Ulrich, R. L., D. Deshazer, E. E. Brueggemann, H. B. Hines, P. C. Oyston, and J. A. Jeddeloh.** 2004. Role of quorum sensing in the pathogenicity of Burkholderia pseudomallei. J. Med. Microbiol. **53:**1053–1064.
44. **Valade, E., F. M. Thibault, Y. P. Gauthier, M. Palencia, M. Y. Popoff, and D. R. Vidal.** 2004. The PmlI-PmlR quorum-sensing system in *Burkholderia pseudomallei* plays a key role in virulence and modulates production of the MprA protease. J. Bacteriol. **186:**2288–2294.
45. **White, N. J.** 2003. Melioidosis. Lancet **361:**1715–1722.
46. **Wuthiekanun, V., M. D. Smith, D. A. Dance, A. L. Walsh, T. L. Pitt, and N. J. White.** 1996. Biochemical characteristics of clinical and environmental isolates of Burkholderia pseudomallei. J. Med. Microbiol. **45:**408–412.

Editor: J. T. Barbieri